

The Performance of Gaseous Electron Multiplier Preamplifiers (GEM) as a Neutron Sensitive Detector

Haitham Abdel Majid

Physics Department

APPROVED:

---

Dr. Tony Forest, Chair, Ph.D.

---

---

# Abstract

I propose to construct and measure the performance of a fission chamber instrumented with preamplifiers known as a Gas Electron Multiplier (GEM). This fission chamber is a chamber filled with a 90/10 Ar/  $CO_2$  gas mixture enclosing U-233 as a neutron sensitive material. A neutron of sufficient energy has the potential to interact with the fissionable material, producing heavy ions known as fission fragments. The fission fragments within 5 microns of the target's surface may escape and ionize the gas in the chamber. Electrons, freed from ionization, will be driven by an electric field toward the GEM preamplifiers to produce secondary electrons. After multiplication by GEM preamplifiers, most of the electrons will end up to a charge collector to provide a pulse to the DAQ-system.

The Gas Electron Multiplier (GEM), invented by Fabio Sauli in 1997.<sup>?,?,?,?</sup> The GEM preamplifier is a 50 micron sheet of kapton that is coated on each side with 5 microns of copper. The copper clad kapton is perforated with 50-100 micron diameter holes separated by 100-200 micron in a staggered array . The GEM detector has been designed, developed and used for detection in CERN since 1997. Fabio Sauli invented the GEM preamplifier in 1997<sup>?,?,?,?</sup> and Gandi and De Oliveira designed it. The design was on 50,5 um kipton copper clad cards, which had holes of 70 um in diameter in a an equilateral triangular pattern with a 140 um pitch distance.

It is worth mentioning the thick gaseous electron multiplier (THGEM) preamplifier design, the macroscopic version of GEM, which represents the next generation of GEM preamplifiers. THGEM preamplifier uses a perforated fiberglass board (PC board) clad with a conducting material. A thick fiberglass sheet, that may have up to 10mm thickness, is perforated with holes with a diameter of 2 mm.

# Motivation

Fast neutron detectors have many applications in different disciplines of nuclear technology. For instance, fast neutron detectors are used in Homeland security applications, such as neutron imaging for large cargo containers; high penetrating neutrons are desirable when efficient fast neutron detectors are available. They are also used for real time measurements of fast neutron beam flux, which is used in nuclear reactors such as the Advanced Test Reactor (ATR). The goal of this research is to economically build and test the performance gaseous electron multipliers preamplifiers, as they are installed in detector's chamber that has a coated layer of fissionable material such as U-233.

# Table of Contents

	<b>Page</b>
Abstract . . . . .	ii
Motivation . . . . .	iii
Table of Contents . . . . .	iv
List of Tables . . . . .	v
List of Figures . . . . .	vi
<b>Chapter</b>	
1 Introduction . . . . .	1
2 . . . . .	2
2.1 Inroduction . . . . .	2
2.2 Radioactivity and Neutron Emission . . . . .	4
2.2.1 Neutron Induced Fission Cross Section and U-233 characteristics . .	6
2.2.2 U-233 Coating . . . . .	8
2.2.3 Escaped fission fragments . . . . .	9
2.3 Ionization . . . . .	10
2.3.1 Energy loss by Charged particles . . . . .	12
2.3.2 Ionization in fission chambers . . . . .	13
2.4 Diffusion . . . . .	15
2.4.1 Electrons and Ions behavior in a gas . . . . .	15
2.5 Electron Multiplication . . . . .	20
2.5.1 Townsend's First Coefficient . . . . .	20
2.5.2 Gas Quenching . . . . .	22

# List of Tables

2.1	.....	2
2.2	The table shows energy range classification of neutron detectors and their characteristics. ....	3
2.3	The table shows a comparison among the common radio-isotopes half lives for spontaneous fission, alpha emission, and neutron emission and those of Cf-252 ....	4
2.4	Minimum ionization energy for different particles pass Ar/CO2 . . . . .	11
2.5	.....	14
2.6	.....	14
2.7	.....	14

# List of Figures

# Chapter 1

## Introduction

Neutron detectors have many applications in nuclear, medical, and industrial fields. Recently, many explorations, new theories and phenomena appeared in detector science, that are related to many applications in different fields. Researchers devote their efforts to studying the best methods in detector design, data collection and analysis, and signal processing, in order to evaluate detector characteristics for use in specific applications. Recently, radiation has applications in many fields, so radiation detectors are widespread in the medical, scientific, and safeguard industries. For instance, there is fast development in the sophistication of airport security detectors. There are a lot of passengers, luggage, and goods entering or leaving the airport that have to pass through inspection. For many reasons, manual inspection is not a solution in this case, but using radiation detectors can help in performing a highly accurate inspection for all that enters or leaves these travel points without delay. Specifically for cargo containers, fast neutrons are used since they are highly penetrating particles and help in counting or imaging to inspect the contents of the containers. Another specific application for detectors is using neutron detectors in nuclear reactors: they are important in determining the reactors stability, and in radiation monitoring in the area surrounding the reactor.

This project represents a study of fast neutron detectors that are based on gaseous fission chambers. The project has detailed discussion in the coming chapters that discuss applications of neutron detectors, and specifically fast neutron detectors, the main concepts and the theories that justify the processes occurring in the fission chamber. The detector's structure and components. The experimental observation and collected data, data analysis and simulations, conclusions, and recommendations for any the future work related to this project.

# Chapter 2

## 2.1 Introduction

There are many types of neutron detectors because of the wide variety of applications; they can be classified depending on the type of interaction, the type of medium that is responsible for producing the signal, the energy range of detected neutrons, or the performance which is determined by calculating their efficiency, energy resolution, sensitivity to gamma particles, detector dead time, and spatial resolution. The following table shows some of the neutron detectors and their structure and energy range.

Signal generated	Material Structure	Neutron Energy (MeV)
Scintillation in Solid	Plastic, Inorganic: LiBaF <sub>3</sub> :Ce	10-170
Scintillation in Liquid	BC501A	0.004- 8.00
Ionization in gas	Ar-CO <sub>2</sub> (90/10), P-10	1 MeV or less

Table 2.1: The table shows neutron detectors phase structure, and their energy range.

The gaseous detector have passed through stages of development to improve signal's width and amplitude. Gaseous detectors started with a gas chamber that contained only a capacitor, a high voltage was applied to collect the ions and electrons after ionization. The disadvantage was the signal of an order of milliseconds, which is very slow for most applications.

So the next step was to make the pulse width shorter; rather than waiting for the electrons to reach the anode, a grid was placed between the cathode and the anode to shorten the distance crossed by the electrons. As a result, the pulse width was improved to the microsecond scale, the new detector was named the Frisch grid detector.

Recently, detectors are developed to be particle counters, time projectors, or used for imaging purposes, so proportional counters, wire chambers, and micro-pattern gaseous detectors (MPGD) were developed to provide these applications with high quality detectors.

The MPGD detectors are the latest the improvement in gaseous detectors; there are many types and patterns for these detectors, which helped to detect the lower ionizing particles that pass through a preamplifier; they provide a high electric field for electron multiplication, the former process improved the signal's width to be of the order of nanoseconds. The following figure shows different patterns of MPGD detectors:

Author	dangendorft	F. Murtas	M. Shoji
Neutron Type	Fast	Fast	Thermal
Converter	polypropylene $n \rightarrow p$	60mm polypropylene	B-10
n-energy (MeV)	2-10	2-20	$0.025 \times 10^{-6}$
FWHM (mm)	0.5-1.0	1.0	1.2
Efficiency	0.05 (2 MeV )	$10^{-4}$ (60 keV)	0.027

Table 2.2: The table shows energy range classification of neutron detectors and their characteristics.



The picture shows different types of MPGD structures.

Building a neutron detector based on GEM electrodes has been done for imaging purposes. There are a few groups that were interested in constructing neutron detectors for imaging. Most of the detectors have a neutron converter based on polyethylene for fast neutrons of energy (1-20 MeV), or B-10 coating for detecting thermal neutrons. The following table shows the properties of the previously built neutron detectors.

In all the previous trials, the detectors had low efficiency for detecting fast and thermal neutrons. The aim of this work is to study and build a neutron detector with a higher efficiency for thermal and fast neutrons by installing U-233 thin film. U-233 is a fissionable material with a high fission cross section for thermal and fast neutron, U-233 will be coated on the cathode surface inside the gaseous chamber, in a way that emits the fission fragment in the drift area of a chamber has three GEM preamplifiers.

The detector operation has successive physical processes that governs its performance. The beginning is a neutron induced **fission** that occurs on U-233 coating surface on the cathode, the fission produces two fission fragments moving back to back; at least one of them will **escape** from the surface of U-233 into the surrounding gas. The fission fragment will **move**, **collide**, and **ionize** the gas, it will **exchange** charge with the medium's atoms and molecules until it becomes neutral, meanwhile electrons will primarily scatter and they mostly **diffuse** in the direction of the drift electric field which guides them to the first GEM preamplifier. If the electron passed through one of the GEM's preamplifier holes, it will accelerate and ionize the surrounding atoms, that will cause electron **multiplication**. Then the number of electron increases creating avalanches, then creating streams. The electrons' track ends when they are collected by charge collector, creating a negative pulse on the oscilloscope display.

Nuclide	$T_{1/2}$ Fission	$T_{1/2}$ $\alpha$ -decay	Neutron/sec.gram
$U_{92}^{235}$	$1.8 \times 10^8$ years	$6.8 \times 10^8$ years	$8.0 \times 10^{-4}$
$U_{92}^{238}$	$8.0 \times 10^{15}$ years	$4.5 \times 10^9$ years	$1.6 \times 10^{-2}$
$Pu_{94}^{239}$	$5.5 \times 10^5$ years	$2.4 \times 10^4$ years	$3.0 \times 10^{-2}$
$Pu_{94}^{240}$	$1.2 \times 10^{11}$ years	$6.6 \times 10^3$ years	$1.0 \times 10^3$
$Cf_{98}^{252}$	66 years	2.65 years	$2.3 \times 10^{12}$

Table 2.3: The table shows a comparison among the common radio-isotopes half lives for spontaneous fission, alpha emission, and neutron emission and those of Cf-252

## 2.2 Radioactivity and Neutron Emission

Radioactive material may emit neutrons, photons, electrons or alpha (ionized He-3) particles, which may either be naturally occurring (intrinsic source) or be a manmade source. Radioactive sources radiates a type or more than one type of particles, as a result of having the radioactive nucleus in a nuclear excited state. In a nucleus transition from the nuclear excited state to a lower excited state or to its ground state, if the particle energy is enough to go over Coulomb barrier, the particle leaves the nucleus with a kinetic energy proportional to the nuclear transition energy and the nucleus Coulomb barrier. In case of the neutron emission, there are many theories that study the emission from semi-classical or quantum point of view; but in summary the neutron has to penetrate the nucleus centrifugal Coulomb barrier, since the neutron is not a charged particle. Also, the process depends on the angular distribution of neutrons and the protons in the nucleus, and the spin of the emitted neutrons. The orientation in the neutron wave function is not as critical a criterion as it is in the case of a proton emission from the nucleus.

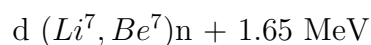
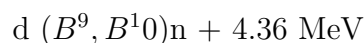
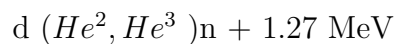
Neutrons are classified into four types depending on their energy; each type has an energy range which may change from one reference to another. The following table shows the types of neutrons, their energy range, and common materials used for detecting them in that range.

Neutron Type	Energy Range	Common detective material(s)
Ultracold Neutrons	$< 10^{-7}$	He-3
Very Cold Neutrons	$2 \times 10^{-7}eV < K.E < 5 \times 10^{-5}eV$	He-3
Cold Neutrons	$5 \times 10^{-5}eV < K.E. < 0.025eV$	He-3
Thermal Neutrons	$K.E \approx 0.025eV$	Be-4, Li-6
Epithermal Neutrons	$1eV < K.E < 0.1keV$	U-235
Intermediate Neutrons	$1 \text{ keV} \geq K.E \leq 0.1 \text{ MeV}$	U-235
Fast Neutrons	$K.E > 0.1MeV$	U-233, U-238, Th-232

table shows the energy classification of the neutrons, energy range of each class, and the appropriate material(s) used for detection

The table below shows radioactive nuclei and their half lives that mainly emit neutrons by spontaneous fission.

In addition to the natural sources, there are industrial neutron sources (extrinsic). There are many ways to produce extrinsic neutron sources, such as a particle accelerator, a Van de Graaff electrostatic accelerator, or a nuclear reactor. When using a particle accelerator, photon activation is one of the methods used to produce these types of sources, by carefully choosing an appropriate target. When a Van de Graaff accelerator is used, it projects a deuteron or a proton toward the target to produce neutrons, for example:



Finally, nuclear reactors are used to produce extrinsic radioactive sources. Nuclear reactors are considered the richest environment for producing most radioactive isotopes, which are commonly used in many fields. In a reactor, many neutron interactions take place to produce different radioisotopes, such as neutron fission, neutron activation, or neutron capture. For example, a neutron induced fission for U-233 is a main source for  $Sn^{117}$ .

### 2.2.1 Neutron Induced Fission Cross Section and U-233 characteristics

The definition of an induced neutron fission cross section is the probability of occurrence of a fission interaction by an incident neutron of a specific energy. Actinides and lanthanides generally have high fission cross sections, compared to those of the rest of the elements in the periodic table. For instance, U-235 and Pu-239, which are thermal neutrons, have 600-700 and 800 barn respectively, while fast neutrons, such as U-238 and Th-232 have 0.1-1 barn as fission cross section when the incident neutron energy range is 1-30 MeV.

There are generally two types of cross sections: microscopic and macroscopic fission cross sections. The microscopic cross section defines the effective area for a single nucleus for an interaction. The macroscopic cross section determines the probability of a neutron to interact when it travels a unit distance in a macroscopic material, its unit is  $cm^{-1}$  (which is the reciprocal of mean free path), it is defined mathematically in terms of the microscopic cross section by::<sup>?,?</sup>

$$\Sigma = n * \sigma$$

Where

$\Sigma$  is the macroscopic cross section and  $\sigma$  is the microscopic cross section , n is the material (target) atomic density (*atom/cm<sup>3</sup>*).

When a neutron flux ( $\Phi$ ) interacts with a material of thickness x, the flux exponentially attenuates inside the material as shown by the formula:

$$\Phi = \Phi_0 \exp -(\Sigma * x)$$

so,

$$\Sigma = -x^{-1} \ln(\Phi/\Phi_0)$$

The microscopic cross section of the material is:

$$\sigma = -\frac{x^{-1}}{n} \ln(\Phi/\Phi_0)$$

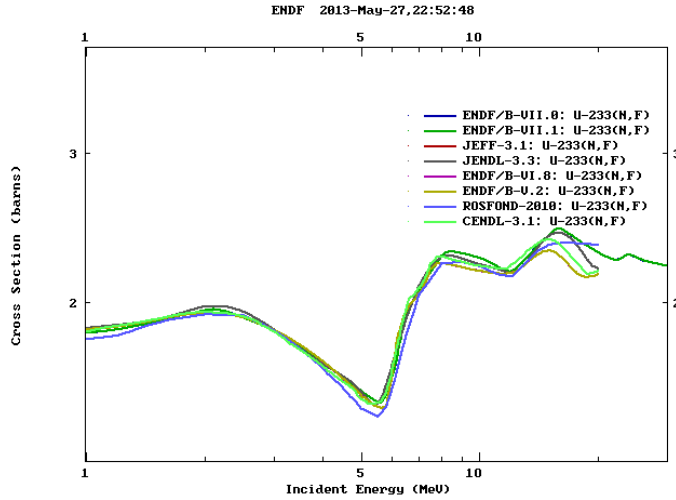
Where  $\Phi$  is the number incident particle per unit area per unit time,  $dN$  is the average number of particles per unit time that interacted per unit solid angle, and  $\Omega$  is the solid angle.

Since the cross section has an area unit (barn), some authors define this quantity as the area to which the particle is exposed, in order to make an interaction.<sup>?,?</sup> The cross section values are represented as a function of energy that gives the value of the cross section for each energy value and shows the resonance peaks. A theoretical description of the neutron fission cross section curve over all energy ranges is not available, but statistically it is possible to evaluate the parameters for an assumption that describes part of the cross section curve within a determined error.

Since there are differences among fission cross sections in different energy ranges, each material has advantages for use in specific applications. For fast neutron detectors, Th-232

or U238 can be used as a sensitive neutron surface coating in the detector.

Indeed, U-233 has a fission cross section that reaches 2 barn for fast neutrons, and up to  $10^4$  barn for thermal neutrons. The figure below shows the fission cross section in the fast neutron range up to more than 30 MeV.



It should be noted that fission cross section curve for U-233 decreases between 5-6 MeV, as a result of the increase in the probability of evaporating a neutron without changing the excitation level of the nucleus. As the incident neutron energy increases, the fission probability increases with a change in the nucleus' excitation level. Another drop in the curve is noticeable between 11 and 14 MeV for the same reason. Tracking the drops in the curve helps in studying the chain fission interaction (n,nf) in U-233 in the shown energy range.

U-233 cross section curve has resonance peaks; most of them appear when the neutron energy is between 10 eV and less than 1 MeV. According to fission cross section categories, U-233 belongs to a category that describes the behavior of fissile nuclei that have a high fission cross section for thermal neutrons.

Another way to look at the U-233 nucleus is by analyzing the parameters that determine the neutron fission cross section such as: the fission barrier energy, activation energy, and binding energy. The following table shows the calculated values of these parameters in MeV unit:

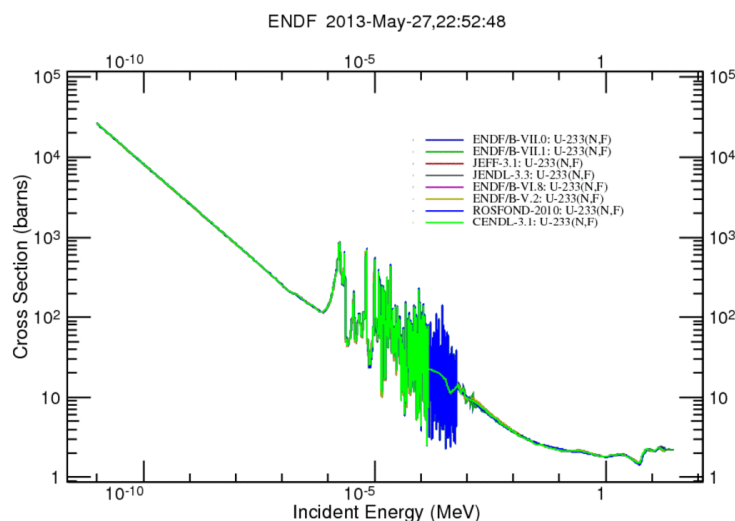
Nuclide	$U_{92}^{233}$	$U_{92}^{238}$	$Th_{90}^{232}$
Coulomb Barrier $E_b$ (MeV)	6.0	6.6	6.9
Activation Energy $E_a$ (MeV)	5.1	5.7	6.0
Neutron Binding Energy (MeV) $B_n$	6.8	4.8	4.9
$B_n - E_a$ (MeV)	1.7	-0.9	-1.1

The table shows a positive difference between Coulomb barrier and the neutron binding energy, which indicates that the fission cross section value for slow neutron is  $\gg 1$ , in the case of U-238 and Th-232 the difference between the binding energy and Coulomb barrier is  $\approx 0.1$ . U-233 fission barrier is 6.0 MeV which made it high enough to avoid any spontaneous

fission events, but less than those of U-238 and Th-232 which increases its fission cross section. These calculations encourage the use of U-233 to be a target for fast neutrons, as will be shown in the next sections.

### 2.2.2 U-233 Coating

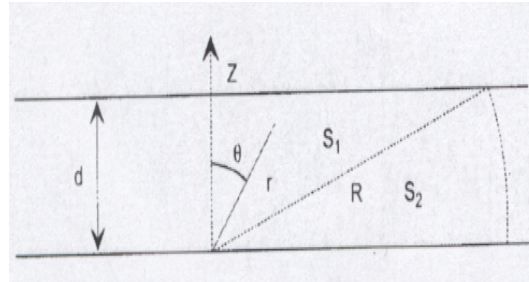
The fission chamber has a U-233 fissionable neutron-sensitive target. The fission chambers usually have target materials that makes them sensitive to neutrons of a specific energy range. The most commonly used material for detecting thermal neutron is U-235, while fast neutrons Th-232 and U-238 represent good targets. In some cases, the fission chamber may contain more than one target to detect a wide range of emitted neutrons.<sup>7</sup>In this work, based on the analysis of the characteristics of U-233 that are discussed in the previous section, and based on the availability of U-233 coat on a metal disk, U-233 is used as a neutron sensitive material in the fission chamber.



U-233 coating is on a circular metal plate which is in a direct contact with the cathode. The coating of U-233 has a circular shape and is an inch in diameter, 20-40  $\mu\text{m}$  in thickness. The U-233 circular plate is glued to a square FR4 copper clad plate 12 cm long, and 1 mm thick, which is placed on the top of the first GEM preamplifier to be the detector cathode; this plate has a hole 4 cm in diameter that keeps the U-233 coating directly exposed to the chamber gas.

**2.2.3 Escaped fission fragments**

U-233 coating sensitivity is relative to incident neutrons when it has an appropriate thickness. Compared to the other neutron sensitive targets, U-233 is relatively sensitive to a wide energy range of incident neutrons; the neutron range may extend from 0.1 MeV to more than 30 MeV. However, the coating thickness determines if a fission fragment can escape from its surface to cause an ionization. In a study aimed at determining the neutron fluence in nuclear reactors, the range of a fission fragment was calculated in  $UO_3$  emulsion, of thickness 0.1  $\mu m$  and density  $7.29g/cm^3$ , is  $12.07 \pm 0.09\mu m$  .<sup>?,?</sup>



Assuming the fission fragment mobility is the same as the  $UO_3$ . As the thickness increases more than 0.1  $\mu m$ , the range will decrease according to the following equation :

$$R = R_T - \langle r \rangle$$

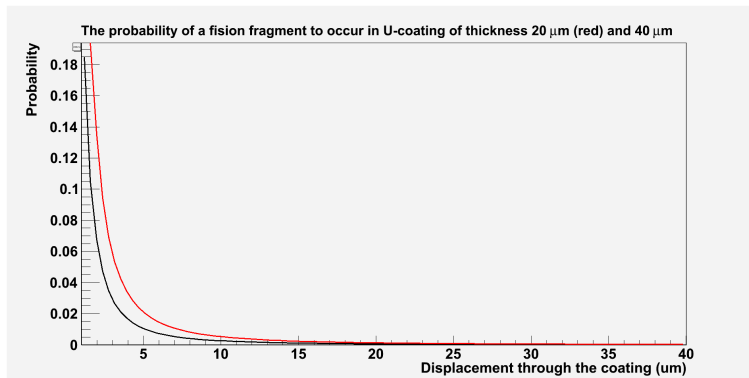
$$\langle r \rangle = \frac{\ln(d/R_T) + 0.5}{2/d(1 - R_T/d) + R_T^{-1}}$$

where  $R_T$  is the mean range of a fission fragment in  $U_3O_8$  emulsion, d is  $UO_3$  coating thickness, and  $\langle r \rangle$  is the average range of the fission fragment in the thin film.

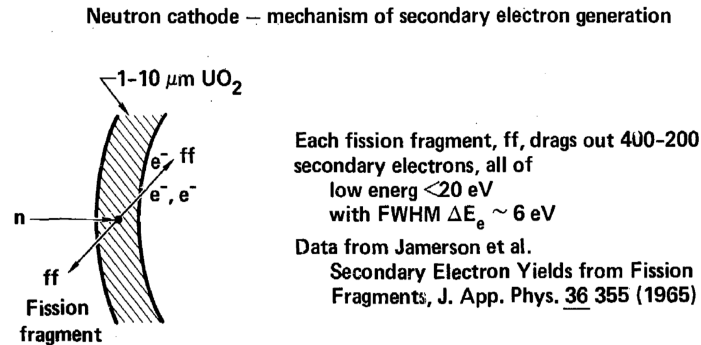
The previous equation is derived from defining the probability of a fission a fission fragment to occur in a distance r with an angle  $\theta$  as the following:

$$Probability = \frac{d}{4\pi r^2 R}$$

The following figure shows the probability values for 20  $\mu m$  and 40  $\mu m$  coating thickness of U-233, the highest probability for a fission fragment to escape to the gas when the fission event occurs within 1  $\mu m$  from the coating surface.



Producing free electrons in the gas will consequently create a signal. Although the fission fragment leaves the surface of U-233 coating and ionizes the gas, the minimum 200 electrons of energy around 20 eV become free through the fission fragment's track in the U-233 coating of thickness 1-10 $\mu\text{m}$ .<sup>?,?,?,?</sup>, separating the low energy electrons from the higher energy ones that are scattered freely from a fission fragment's ionization is beyond the scope of this research.



## 2.3 Ionization

Historically, ionization has been discussed as a classical then as a quantum phenomenon. One of the first studies for ionization was by Townsend, who experimentally defined the Townsend first coefficient to describe ionization and electron multiplication. In later studies, the Townsend first coefficient was theoretically evaluated by comparing the monopole and the dipole solution for the scalar Maxwell-Boltzmann equation, as electron diffusion is minimized, and without electron attachment, so the Townsend first coefficient was written as the following:<sup>?</sup>

$$\alpha_T = 2\lambda_L\alpha_i/(\eta + \lambda_L)$$

where

$\alpha_T$  is Townsend first coefficient, and  $\alpha_i$  the ionization coefficient without attachment from Maxwell-Boltzmann equation.

$\lambda_L = W/D_L$ ,  $W$  is the drift velocity, and  $D_L$  is the longitudinal diffusion coefficient (considered toward the  $z$ -axis).

$$\text{and } \eta = \lambda_L^2 + 2\lambda_L\alpha_i$$

Defining  $\alpha_T$  by the first equation is important in the gas breakdown interpretation, and calculating the mean rate of ionization per electron.<sup>?</sup>

The quantum approach for ionization starts by considering the modern picture for the atom, a nucleus surrounded by electron clouds. Each electron state is defined by specific quantum numbers, to distinguish the electron quantum state from any other state. If an

Type of particle and its energy	Energy per ion-electron pair (eV)
9 keV x-rays	27.9 $\pm$ 1.5
10 keV electrons	27.3
40 keV electrons	25.4
(5-25 keV) x-rays Ar-37(K-capture) and beta	27.0 $\pm$ 0.5
7.68 MeV alpha	26.25
340 MeV proton	25.5

Table 2.4: Minimum ionization energy for different particles pass Ar/CO2

electron gains energy, the electron will be in a higher excited state, and then it will be back to its original state after radiating a photon, or to another state if an EM radiation spectrum (photons with different energies) is observed in case of the Auger effect. So, the ionization definition, based on the quantum approach, is the liberation of an electron from the medium's atoms or its molecules' confinement. The minimum amount of energy required to liberate the electron is referred to as the ionization energy, and it is approximately specific for all types of particles. When the ionizing particle gets into the medium, its deposit of energy scatters free electrons; they get their kinetic energy after losing part of their energy when releasing from the atom confinement, then pass through the medium facing different electron-electron collisions. The number of free electrons can be estimated for a charged particle using the Bethe-Block equation, as will be shown in the next section. As an example of ionization in a gas, when a fission fragment ionizes the Ar/CO2 gas, a free electron will get kinetic energy, depending on the fission fragment's energy loss and the number of collisions the electron passes through.

Ionization is a stochastic process: it depends on the elastic and inelastic cross sections, as determined by the medium type, the ionizing particle energy, and mass (heavy or light in case of fission fragments). However, as mentioned previously, the amount of energy needed to have an ionization event is about the same, regardless of the incident particle type or energy as shown in the following table for argon gas.<sup>?, ?, ?, ?</sup>

Ionization is an essential process that should occur in the detector through and after the particle passage. In order for the gaseous detector principle to work, ionization must be present, so the observer will have an indicator for the particle inside the detector. Though the ionization happens in order to release the primary electrons at the time of particle passage, it continues to be responsible for the secondary electrons and the electron multiplication, as will be discussed in the coming sections.

### 2.3.1 Energy loss by Charged particles

Fission fragments are a source of ionization when they penetrate an Argon gas chamber. The energy used for such an event is highly dependent on the fission fragment mass and velocity. At low fission fragment velocities, recoiling becomes a competitive process that decreases the probability of ionization. In the case of high velocity, the probability of ionizing the gas increases. The theoretical study of the energy loss of fission fragments is through three steps; as the fission fragment is totally ionized, as the fission fragment is exchanging the charge with the gas atoms, and as the fission fragment is totally neutralized.

The total energy of a fission fragment without a bound electron is given by

$$E = \frac{kZ_1Z_2e^2}{r} + \frac{1}{2}Mv^2$$

where  $Z_1, M$  and  $v$  are: the atomic number, the mass and the velocity of the fission fragment directly after the fission reaction,  $Z_2$  is the atomic number of the gas atom. The Coulomb force represents the repulsion force between the ionized gas atoms and fission fragments, as well as the attraction force between the fission fragment and electrons. The second term in the above equation dominates until the fission fragment begins to probe the charge within the neutral ionization gas atoms.

When the fission fragment decelerates, a charge exchange starts between the fission fragment and gas atoms, as the electrons are either scattering away from the fission fragment or attaching to it. The total energy loss of the fission fragment suggested by Bohr in 1940 is given by the following:<sup>5</sup>

$$\frac{1}{N} \frac{dE}{dx} = \frac{4\pi e^4}{mv^2} (Z_1^{eff})^2 Z_2 \log \frac{1.123mv^3}{we^2 Z_1^{eff}} + \frac{4\pi e^4}{M_2 v^2} Z_1^2 Z_2^2 \times \log \left( \frac{M_1 M_2}{M_1 + M_2} \frac{v^2 a_{12}^{scr}}{Z_1 Z_2 e^2} \right)$$

where  $N$  is the number of particles of the stopping medium per cubic centimeter,  $M_1, M_2$  are masses of the fragment and the absorber,  $Z_1, Z_2$  are the atomic numbers of the fragment and the absorber,  $e$  is the electron charge,  $v$  is the fragment velocity,  $Z_1^{eff}$  is the effective charge of the fragment; it changes from 20 at the beginning of the fission fragment track to a value of 2 close to the end of it.<sup>5</sup>  $a_{12}^{scr}$  is an impact parameter which indicates at what distance the energy loss in nuclear collisions is effectively zero, owing to the screening of the charges of the nuclei by the atomic electrons;  $w = I/\hbar$  is the average oscillation frequency of the electrons in the atom.

This formula is an initial estimation of the total energy loss by the fission fragment under each stage of charge carrier exchange between the fission fragment and the gas atoms; it relies on how well the Z-effective is estimated at each ionization stage. Consequently, the first term is dominant in the beginning of the interaction between the fission fragment and the ionization gas, while the second term dominates close to the end of the fission fragment's track.<sup>5</sup>

The Bethe Bloch equation is commonly used to estimate the energy loss for charged particles, including fission fragments. It involves the use of a diverse model for the effective

charge obtained, based on experimental data analysis for energy loss data<sup>6</sup>

$$-\frac{dE}{dx} \left[ \frac{\text{MeV}}{\text{mg/cm}^3} \right] = 3.072 \times 10^{-4} \left( \frac{Z^{eff}}{\nu/c} \right)^2 \left( \frac{Z_m}{A_m} \right) \ln \left( \frac{m_e \nu^2}{I} \right)$$

where  $Z_{eff} = Z \left[ 1 - A \exp \left( -B \frac{\nu}{\nu_o Z^{\frac{3}{2}}} \right) \right]$

$Z$  is the nuclear charge of the fission fragment,  $\nu_o$  is the speed of the electron in first Bohr orbit,  $\nu$  is the speed of the ion,  $Z_m, A_m$  are the nuclear charge and the atomic mass of the medium,  $m_e$  is the mass of the electron,  $I = K Z_m$  is the mean excitation energy of the atomic electrons of the medium of atomic number  $Z_m$ .  $A, B$  are the fitting parameters dependent on the medium, for example  $A=0.92, B= 0.72$  for light fission fragments.  $A=0.99, B= 0.82$  for heavy fission fragments as they are passing  $\text{Ar}/\text{CH}_4$  (95/5) medium.?

Furthermore, the Bethe-Bloch equation is modified to include relativistic charge particles' energy loss but they will not be considered in this work, since its scope is focused on calculating the energy loss for alpha particle decay from U-233, which will have a maximum energy of 8.4 MeV, or for fission fragments that are emitted from a fission reaction which have only enough energy to move them a distance of a micrometer range in  $\text{Ar}/\text{CO}_2$  gas.

The final step describes the fission fragment ionization when it becomes neutrally charged by collecting electrons from the medium. The probability of ionization is very low during this step, because of the fission fragment's neutral charge and low kinetic energy. The lowest energy at which a fission fragment can ionize a gas is expected to be equivalent to the energy of its weakest bound state electron, which can be between 15.7 eV and 3.2 keV. In more specific studies that are based on classifying the fission fragments into light and heavy fission fragments, the researchers tried to measure the amount of fission fragment energy consumed by processes other than ionization. The energy is referred to as the ionization defect energy  $\Delta E$  (ionization defect)<sup>1</sup>

$$\Delta E = E - I w_\alpha$$

where  $E$  is the energy of the primary particle,  $I$  is the number of ionization events, and  $w_\alpha$  is the amount of energy used to produce an ion pair.

Light fission fragments have a measured  $\Delta E$  of 2.5 MeV when their initial energy was 67 MeV,<sup>1</sup> and heavy fission fragments have a measured  $\Delta E$  of 4.2 MeV when their average initial energy was 98 MeV.<sup>1</sup> These observations define "ionization defect" energy which experimentally indicates that ionization energy is actually higher than that of the least bound electron binding energy, but the fission fragment is unable to make any additional ionization in the medium.

### 2.3.2 Ionization in fission chambers

Ionization by a fission fragment is not the only source for free electrons which may cause a signal in a fission chamber. Fission chambers usually contain neutron-fissionable materials;

nuclide	Energy Minimum	Energy Maximum (keV)
U-233	25	1,119
Ra-225	40	40
Ac-225	10.5	758.9
Fr-221	96.8	410.7
At-217	140	593.1
Bi-213	323.81	1,119.4

Table 2.5:

Nuclides	energy (MeV)	half life
$Ra^{225} \rightarrow Ac^{225}$	0.357	14d.
$Bi^{213} \rightarrow Po^{213}$	1.426	46min.
$Tl^{209} \rightarrow Pb^{209}$	1.981	2.2 min.
$Pb^{209} \rightarrow Bi^{209}$	0.644	3.25h
$Bi^{209}$	1.893	stable
caption		

Table 2.6:

there are heavy radioisotopes that decay and emit more than one type of the ionizing radiation, by the mother nucleus or by its daughters. For instance, when the fission chamber contains U-233, although U-233 is mainly an alpha source, it may have ionization events that are caused by fission fragments (in case of neutron exposure), alpha particles, beta particles, or gamma rays. More specific details about U-233  $\gamma$ -decay energy spectrum is shown by the following tables:

For  $\beta$  – decay :

and for  $\alpha$  – decay :

Generally, there are other physical processes occurring in the gaseous medium, which are directly related to the gas mixture's chemical structure such as: photoionization, thermal ionization, deionization by attachment (negative ion formation) , photoelectric emission, electron emission by excited atoms, penning, and field emission. The previous processes

nuclide	Energy (MeV)
Pb-213	8.4
Bi-213	5.9
At-217	6.3
Fr-221	6.3
Th-229	4.85 (alpha spectrum, highest counts for is 4.85 MeV)
caption	

Table 2.7:

may factor in decreasing or increasing the number of free electrons in the medium; some of processes used to calculate the electron number in the Maxwell-Boltzmann equation as will be mentioned in the next section. Without computer simulation, evaluating the number of free electrons before and through preamplification becomes complicated for different media, if more than one of the latter processes is going to be considered. The Garfield software package simulates ionization in the gas mixture, it considers all the former physical processes, and has the ability to simulate the electrons' multiplication by GEM preamplifiers, it accepts external solutions for the electric field by other software packages like ANSYS, and it has more than one package such as Magboltz, HEED, and Imonte 4.5, which can be used for more precise simulations as will be shown by the simulation chapter.

## 2.4 Diffusion

### 2.4.1 Electrons and Ions behavior in a gas

?,?

Studying diffusion and mobility of charged particles in a gas is different for ion than those of the electron. Diffusion and mobility are conceptually similar for all charged particles that are dependent on the Maxwell-Boltzmann equation. However, there are differences in the differential equation constraints if the equation is for an ion or for an electron: first, the ratio between the mass of an electron to that of an ion is very small; if a few eV work is spent by the electric field, the electrons will gain a high velocity compared to that of the ions if they are all accelerated under the same electric field. Also, the probability of low energy electrons to make an interaction is higher than that of the low energy ions, especially when the electron interactions are supported with accurate calculations for their drift velocity (stream group velocity). Electrons at low energy have the ability to produce vibrations and excitations in the gas atoms or molecules which are measured within the lab frame, but low energy ions have very low cross sections for most interactions with gas atoms or molecules; when ion interactions happen, a complexity appears in measuring the ion interactions' motion parameters, but in the case of the calculations for electrons, they are simpler for the velocity distribution in many gases, since the ratio between a gas atom mass and an electron mass is always very small. Furthermore, there are many interactions responsible for producing electrons, such as thermionic emission, photoemission, or radioactive decay. On the other hand, creating an ion requires electron bombardment, photo-ionization or an electric discharge, which requires more sophisticated conditions for the experiment, as the free ions are not as sensitive as electrons to the non-uniformity of the electric field, electric potential and magnetic field. Finally, the existence of the impurities is always a concern; the ions lose most of their energy in the molecular level, and the electron energy loss is within the atomic level in a gas. As a result, the ionic velocity distribution is not affected by the existence of these impurities, except for some cases related to highly accurate ionic studies in gases.

Electron Diffusion

Charged particles' diffusion in gas is defined as the dispersion of the particles in a gas "in which there is a net spatial transport" of the charged particles "produced by a gradient in their relative concentrations". Assuming that the charged particles are localized in a gas with a uniform temperature, pressure and have low  $n$  charged particle density to ignore the Coulomb force.

$$\mathbf{J} = -D\nabla n$$

where  $D$  is the diffusion coefficient and  $\mathbf{J}$  is the number of the charged particle flow per unit time.

The solution of the Maxwell Boltzmann equation describes  $n$  as a function of position  $\mathbf{r}$  and time  $t$ . In our case,  $n$  represents the number electrons propagating in the presence of an electric field. The Maxwell Boltzmann equation is "the equation of continuity for the population  $n f d\mathbf{r} d\mathbf{c}$ " where  $f$  is velocity distribution function. The equation includes the loss of electrons as they transport across a surface boundary in a volume element  $d\mathbf{r}$ , and the effect of the uniform electric field in accelerating each  $n d\mathbf{r}$  electrons which changes  $d\mathbf{c}$  from point to another in the phase space, so the number of point loss in a time  $dt$  is

$$dt \nabla \cdot \left( \frac{n f e E}{m} \right) d\mathbf{c} d\mathbf{r}$$

in addition to the loss of points  $\Delta n$  in  $d\mathbf{c}$  as result of the quasi discontinuous change in position  $\Delta \mathbf{c}$  in velocity space as the electron meets a molecule.

The Maxwell Boltzmann equation can be written based on the previous assumptions as the following:  $?, ?, ?, ?, ?, ?$

$$\frac{\partial}{\partial t}(nf) + \nabla \cdot (nf\mathbf{c}) + \nabla \cdot \left( nf \frac{eE}{m} \right) + S = 0$$

The previous equation is called the scalar equation of the Maxwell Boltzmann equation, it can be written in terms of diffusion coefficients and the average velocity of the electrons; it as shown below:

$$\frac{\partial}{\partial t}(nf_0) + \frac{e}{3} \nabla \cdot (nf\mathbf{1}) + \frac{1}{4\pi c^2} \frac{\partial}{\partial c} (\sigma_E - \sigma_{coll}) = 0$$

**Assumptions:****Velocity Shells**

The electrons are distributed in the phase space in a velocity shell of mean velocity  $\mathbf{W}$ , represented by the following equation

$$W = \frac{\sum_c n_c W(c)}{n dr}$$

Where  $\mathbf{W}(c)$  is the resultant velocity of the velocities of the electrons in the velocity shell  $4\pi c^2 \sin\theta dc d\theta d\phi$ , so the population of velocity points in the shell is represented by the  $n dr [c^2 dc] [f(c, \theta, r, t) \sin\theta dc d\theta d\phi]$ . the following distribution function is assumed for a velocity shell:

$$f(c, \theta, r, t) = f_0(c, \theta, r, t) + \sum_{k=0}^{\infty} f_k(c, \theta, r, t) P_k(\cos\theta)$$

$P_k(\cos\theta)$  is the Legendre polynomial of order k. In the case when the mean velocity is independent of the azimuthal angle, then its magnitude can be determined by the following:

$$W(c) = \frac{1}{n_c} (n dr) c^2 dc \int_0^\pi \int_0^{2\pi} (f_0 + \sum_1^\infty f_k P_k(\cos\theta)) c \cos\theta \sin\theta d\theta d\phi = \frac{c f_1}{3 f_0}$$

and the population density point is :

$$n_c = (n dr) c^2 dc \int_0^\pi \int_0^{2\pi} (f_0 + \sum_1^\infty f_k P_k(\cos\theta)) \sin\theta d\theta d\phi = n f_0 4\pi c^2 dc dr$$

So the mean velocity is evaluated, depending on the former definition:

$$W = \frac{\sum_c n_c W(c)}{n dr} = \frac{c f_1}{3 f_0}$$

It is worth mentioning here that  $W$  represents the mean velocity of the electron population and the instantaneous velocity of the centroid of  $n$ .

**The loss and the gain in the number of points**

The loss in the number of points from  $(c, dc)$  is depending on  $\sigma_E(c)$  and mathematically can be written as  $dt dr dc \frac{\partial}{\partial c} \sigma_E(c)$ . Simultaneously, the gain in the number of points  $(c, dc)$  is evaluated using  $\sigma_{coll}(c)$  such that  $dt dr dc \frac{\partial}{\partial c} \sigma_{coll}(c)$  is the gain per unit volume (in phase space) per unit time.

So the net change in the number of points in the shell is  $dt dr dc \frac{\partial}{\partial c} (\sigma_E(c) - \sigma_{coll}(c))$ .

Where

$$\sigma_{coll}(c) = 4\pi n c^2 \nu_{el} \left( \frac{m}{M} c f_0 + \frac{\bar{C}^2}{3} \frac{\partial f_0}{\partial c} \right)$$

and

$$\sigma_E(c) = \frac{4\pi}{3} c^2 \frac{eE}{m} n f_1$$

$$\nu_{el} = Nc q_{el}(c)$$

$N$  is the molecular density,  $M$  is the mass of the molecule,

$q_{el}(c)$  is the momentum transfer cross section for elastic encounters. and  $\bar{C}^2$  is the mean square speed of the molecules.

### Drift velocity and diffusion coefficients

The electron density number, diffusion coefficients and drift velocity relationship is studied for a close chamber containing a traveling swarm of electrons in a uniform electric field, which directed the swarm toward the  $+z$  axis. Mathematically the relationship is assumed as the following:

$$\frac{\partial}{\partial t} n - D \nabla^2 n + W \frac{\partial}{\partial z} n = 0$$

where

$D = 4\pi \int_0^\infty \frac{c^2}{3\nu} f_0 c^2 dc$ ,  $\nu$  represents "effective collision frequency for the momentum transfer",

$f_0$  is the independent of  $\mathbf{r}$  for a uniform stream that has elastic collisions. In this case,

$f_0$  is a special form of a general form represented by the following equation:

$$f_0 = A \exp \int_0^c \frac{cdc}{V^2 + C^2}$$

As a result, substituting the main formula in the scalar form of Maxwell Boltzmann in the absence of the magnetic field and in a uniform electric field  $\mathbf{E}$ , we get the following formula:

$$\frac{\partial}{\partial t} n - D \left( \frac{\partial^2}{\partial x^2} + \frac{\partial^2}{\partial y^2} \right) n - D_L \frac{\partial^2}{\partial z^2} n + W \nabla_r n = 0$$

$D$  is not isotropic as the  $eE$  force is applied and is defined in the equation above,  $\mathbf{W}$  is represented by the following:

$$W = -\frac{4\pi}{3} \left( \frac{e}{m} \right) \left( \frac{E}{N} \right) \int_0^\infty \frac{c^2}{q_m(c)} \frac{df_0}{dc} dc$$

For electrons moving along the  $z$ -axis:

$$-\frac{\partial}{\partial t} n + D \left( \frac{\partial^2}{\partial x^2} n + \frac{\partial^2}{\partial y^2} n \right) + D_L \frac{\partial^2}{\partial z^2} n - W \frac{\partial}{\partial z} n = 0$$

$$W = -\frac{4\pi}{3} \left( \frac{e}{m} \right) \left( \frac{E}{N} \right) \int_0^\infty \frac{c^2}{q_m(c)} \frac{df_0}{dc} dc$$

$$\sigma_{coll}(c) = 4\pi n c^2 \nu_{el} \left( \frac{m}{M} c f_0 + \frac{C^2}{3} \frac{\partial f_0}{\partial c} \right)$$

$$\sigma_E(c) = \frac{4\pi}{3} c^2 \frac{eE}{m} n f_1$$

$$\nu_{el} = N c q_{el}(c)$$

### The solution of the Boltzmann Equation for a steady stream of electrons originated from a small hole in a metal

The Boltzmann equation has an asymptotic solution for a stream of electrons originated from a hole in a metal plate extending over the plane  $z=0$ ; the hole is at the origin. This solution considers all the conditions mentioned previously, when  $S = 0$ . In the solution, the electron stream travels toward the  $+z$  axis in a uniform electric field, and the velocity distribution only has the first two terms  $f_0 + f_1$

The scalar Boltzmann equation can be written for electron streams moving in the  $+z$ -direction as :

$$\left( \frac{\partial^2}{\partial x^2} + \frac{\partial^2}{\partial x'^2} \right) n + D_L \frac{\partial^2}{\partial z^2} - -W \frac{\partial}{\partial z} n = 0$$

The solution is :

$$n = \exp \lambda_L z \sum_{k=0}^{\infty} A_k r'^{-1/2} K_{k+1/2}(\lambda_L r') P_k(\mu)$$

$$r'^2 = \sqrt{x'^2 + y'^2 + z'^2}, \text{ with } x' = \left( \frac{D_L}{D} \right)^{1/2} x,$$

$$y' = \left( \frac{D_L}{D} \right)^{1/2} y$$

$$2\lambda = \frac{W}{D_L}$$

$K$  is modified Bessel function,  $\mu = \cos\theta$ .

The asymptotic solution for a distance  $r$  from the source, where the spatial gradient has become relatively small. The electron stream has a close surface that contains all the electrons;

$$n_0 = \int n(r, t) dr$$

so  $n(r, t)$  anywhere else is zero.

Considering the monopole and the dipole terms, the solution can be written as the following:

$$\frac{1}{r \sin\theta} \frac{\partial}{\partial \theta} \sin\theta \frac{\partial V}{\partial \theta} = R_k(r') \frac{d}{d\mu} \left[ (1 - \mu^2) \frac{dP_k(\mu)}{d\mu} \right]$$

In the case of the electron stream in GEM preamplifiers, the Boltzmann equation becomes more complicated by adding the other physical processes (inelastic and elas-

tic collisions so  $S$  does not equal zero) and as the electric field is not uniform inside the holes. Therefore, as mentioned previously, computer simulation is a solution that is closer to the real situation of the electron stream in a triple GEM-based detector.

## 2.5 Electron Multiplication

Generally, most gases are neutral in a low electric field, under standard room temperature and pressure. Gases' atoms and molecules tend to stay in the lowest energy level, so the number of collisions among the atoms and molecules is relatively low at standard conditions for temperature and pressure in an area of a low electric field. Those collisions which do occur will cause a low ionization in the medium, down to  $10^{-16} - 10^{-17} A/cm^2$  (including the ionization by the cosmic rays). Changing any of these factors may increase the ionization of a gas. This section will discuss the effect of changing the electric field distribution in the medium on the number of free electrons in a gas. In the fission chamber, the electric field is going to be produced by three GEM preamplifiers; each preamplifier is considered a stand-alone stage for electron multiplication. As an electron pass through the hole, its drift velocity will increase every time it passes through one of the GEM preamplifiers, which increases the number of free electrons in a gaseous medium, as will be shown next.

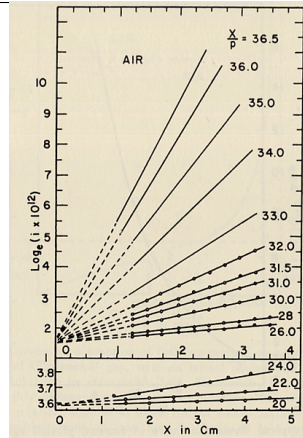
### 2.5.1 Townsend's First Coefficient

Townsend's first coefficient is defined as "the number of new electrons produced by an electron per unit length in the direction of the electric field".

Historically, Townsend started his investigations about discharge in gases, after the fundamental studies, which were conducted around 1899. These studies concentrated on: gas conductivity production by x-rays, diffusion coefficients, mobility of ions, and ion-electron recombination. It was observed that, for an increment in the electric field  $E$  and pressure  $p$  beyond the saturation current value, at some critical value of  $E$  and  $p$ , the current increases rapidly and leads to a breakdown of the gap, which forms a spark.<sup>?, ?, ?, ?</sup> Townsend studied the relationship between  $E/p$  as a function of  $x$ , where  $x$  is the separation distance between the plates. His study was based on the photoelectron emission from the cathode by ultraviolet light in a highly uniform electric field up to 30kV/cm and 1 atm pressure. He plotted different values for  $E/p$ , and found that the slope of the line is  $\alpha$  which is "the number of the new electrons created by a single electron in 1 cm path in the field direction in a gas at appropriately high  $E/p$ ". When Townsend plotted  $\frac{i}{i_0}$  against the distance of separation  $x$ , he concluded the following equation:

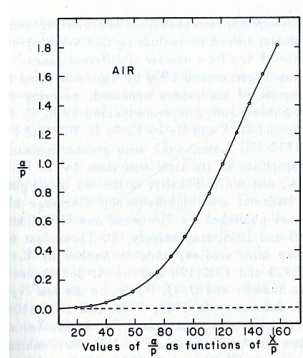
$$\ln\left(\frac{i}{i_0}\right) = \alpha x$$

to calculate  $\alpha$  (the slope) for different values of  $E/p$  as shown in the figure:



Relationship between  $\alpha$  and the distance  $x$  for different values of  $E/p$

Townsend studied  $\alpha$  as a function of  $E/p$  for a given gas, and found that for different values of  $p$ ,  $\alpha$  is experimentally different from the expected calculated value, but the plots match when they represent the relationship between  $\alpha/p$  as a function of  $E/p$ , as shown in the figure below.



Shows  $\alpha/p$  coincides with  $E/p$

The relationship between  $\alpha/p$  and  $E/p$  is shown below. The equation can not predict all the values of  $\alpha/p$  accurately for different values of  $E/p$ , i.e having a single analytical function to fit the experimental results for a gas does not exist, because  $\alpha/p$  is dependent on the number of electrons produced, and the electrons' number changes with changing the average energy distribution of the ionizing electrons.

$$\frac{\alpha}{p} = Ae^{\left(\frac{-BP}{E}\right)}$$

One of the ways to mathematically evaluate  $\alpha/p$  as a function of  $E/p$  is by the kinetic theory. The kinetic theory describes the gas atoms and molecules' energy and their collision rates depending on the mean free path of ionization. It defines the average mean free path by:

$$\bar{\lambda} = \frac{kT}{p\sigma_i}$$

where  $\sigma_i$  is the ionization cross section.

$$\alpha = -\frac{f'(x)}{f(x)} = 1/\bar{\lambda} e^{\lambda_i/\bar{\lambda}} \quad f'(x) = e^{-x/\bar{\lambda}}$$

$x$  is the distance traveled by the electron. Substituting the value of  $\lambda$ , then

$$\frac{\alpha}{p} = \frac{\sigma_i}{kT} e^{-\sigma_i/kT(V_i/(E/p))} = A e^{-B/(E/T)}$$

and

$$A = \frac{\sigma_i}{kT} \quad \text{and} \quad B = \frac{\sigma_i V_i}{kT}$$

The values for  $A$  and  $B$  do not always agree with the experimental values; Kuffel/ $i$ . It is assumed that if the electron energy is greater than  $eV_i$ , it will cause an ionization. However, the ionizations' probability does not always increase with the increase of electron energy. Also, the mean free path is defined as independent of the electron energy, which is not always true.

Since the increase in voltage for electron multiplication does not reach the gas breakdown limit, the electric field increases the number of electrons without producing any discharge. At this point, Townsend's second coefficient does not have an effect on the number of electrons which are produced by the electric field.

### 2.5.2 Gas Quenching

Gas quenching is a non-ionizing process occurs when a gas impurities' molecules have cross sections for excitation and vibration states, instead of ionization for an incident charged particle energy. Gas mixtures usually consist of gas atoms as a main source of electrons and other gas molecules (quenching gas); when an ionization event occurs, free electrons start scattering in the medium. If the scattered electrons have energy exceeding the ionization energy threshold, they will create ionization events, but only vibration will be produced if those electrons interact with impurities' molecules, so they will either trap the electron or decrease to create any further ionization. So by quenching, the number of secondary electrons becomes less, and a higher voltage is required to get a gain from the gas mixtures, compared with a medium that purely consists of one type of atoms.<sup>?,?,?</sup>

Not only does the quenching process decrease the electron energy, but it also decreases the positive ions' energy (produced by ionization), when the ions collide with gas molecules and emit one or more photons from their positive ions. These photons represent the energy loss in a form other than ionization, such as an argon escape peak (when using Argon gas).

Gas quenching can be measured experimentally by evaluating Townsend's first coefficients  $A, B$  for different gas mixtures. The following table represents the Townsend's first coefficients for different ratio of Ar/CO<sub>2</sub> gas mixtures:

Percentage of CO <sub>2</sub>	3.7	22.8	87.2	100
A $cm^{-1}Torr^{-1}$	5.04	221.1	158.3	145.1
B $Vcm^{-1}Torr^{-1}$	90.82	207.6	291.8	318.2
$\frac{E}{p}$ $Vcm^{-1}Torr^{-1}$	16.2	21.6	32.9	36.4

The electric field-pressure ratio in the last row of the above table is in the upper limit of the reduced electric field, which Townsend's equation fits, if E is considered a uniform electric field.

# References

- [1] J.M. Valentine C.Curran. Average energy expenditure per ion pair in gases and gas mixtures. *Reports on Progress in Physics*, 21(1):1–29, 1958.
- [2] A.Bressan et al. High rate behavior and discharge limits in micro-pattern detectors. *NIM A*, 424(2-3):321–341, 1999.
- [3] F. Sauli et al. Gem: A new concept for electron amplification in gas detectors. *NIM A*, 386(2-3):531–543, 1997.
- [4] G. Agocs B. Clark P. Martinego R. Oliveira V. Peskov gand P. Picchi. Developments and the preliminary tests of resistive gems manufactured by a screen printing technology. *JINST*, 3(P020112), 2008.
- [5] K. Hyde, Perlman I., and G.T. Seaborg. *The Nuclear Properties of the Heavy Elements: Fission phenomena*. The Nuclear Properties of the Heavy Elements. Dover Publications, 1971.
- [6] V.A. Rycov. Charge equilibrium emergence of fission fragments after from a solid into gas. *Atomic Energy*, 83(1):321–341, 1997.
- [7] JP Holtzhausen Dr WL Vosloo. *High Voltage Engineering Practice and Theory*. CRC Press, 2000.